Proceedings of the IASTED International Conference
Modelling, Identification and Control (MIC 2017)
February 20 - 21, 2017 Innsbruck, Austria

CFAR DETECTION IN A PASSIVE COHERENT LOCATION SYSTEM USING FM SIGNALS

Dong-Gyu Kim, Geun-Ho Park, Ho Jae Kim, Jin-Oh Park*, Won-Jin Kim*, Jae Heon Ko*, Hyoung-Nam Kim©
Pusan National University, LIG Nex1*
Busan/Korea, Seongnam/Korea*
hnkim@pusan.ac.kr©

ABSTRACT
Recently, interest in a passive coherent location (PCL) system using commercial broadcasting signals has been increased since it exploits the existing broadcasting facilities without revealing the receiver's location. To estimate positions of multiple targets by using the PCL system, constant false alarm rate (CFAR) detection, whose input is the samples of the range-Doppler map, has to be preceded, so that the parameters of the CFAR detector are influenced by the range-Doppler map. However, the characteristics of the range-Doppler map vary with bandwidth of the used broadcasting signals and its collection time. Therefore, algorithm parameters for the CFAR detector have to be properly determined considering those characteristics. To achieve this goal, we analyze the range-Doppler map in a PCL system using commercial FM broadcasting signals and then derive mathematical descriptions for the algorithm parameters of the number of window cells and that of guard cells. We also present which axis out of the range and the Doppler axes is better for CFAR detection.

KEY WORDS
"PCL system" "Passive radar" "CFAR detector" "FM broadcasting signal" "Range-Doppler map"

1. Introduction

A passive coherent location (PCL) system has been used to find unknown multiple moving targets while the detectors are able to hide their locations by not transmitting any signals and only by utilizing the commercial broadcasting signals for a variety of application areas, such as fence-type radar, in-door monitoring, and air-traffic control [1-3] . Among various broadcasting signals, FM analog signals are most frequently considered due to its wide detection coverage [4-5].

Range and Doppler measurements, which are used in the PCL system for finding the location and velocity of the moving targets, can be acquired from the range-Doppler map. The range-Doppler map is obtained by performing cross-correlation between a direct-path signal which is received from broadcasting station to PCL receiver and target echo signals which are reflected by targets propagating to the receiver. Since the peak points on the range-Doppler map are generated at range and frequency difference between the direct signal and the target echo signals, multiple peak points generated by multiple targets should be found to extract the Range-Doppler information.

Constant false alarm rate (CFAR), which is a well-known detection algorithm processor, is commonly used to find multiple peak points on the range-Doppler map [6]. The CFAR processor consists of window cells to determine the threshold, guard cells to avoid the effect of near value of the peak points, and a test cell to confirm whether the targets exist or not. Since the numbers of window and guard cells make an influence on the performance of the CFAR detector, the algorithm parameters, such as the numbers of window cells and the number of the guard cells, have to be adequately determined. Also, the CFAR processor can be conducted based on one out of the range axis and the Doppler axis according to the designer's choice because a range-Doppler map is 2-dimensional data. Thus, to determine the algorithm parameters above, it is necessary to analyze the range-Doppler map based on FM signals.

In this paper, to determine the adequate algorithm setting of the CFAR processor in a PCL system using FM broadcasting signals, we analyze a range-Doppler map considering the signal parameter such as bandwidth and collection time. Then it is shown that the range axis has better detection performance compared to the Doppler axis for the CFAR processor. We also present a mathematical description on the algorithm parameters of the numbers of window and guard cells. Thus, the algorithm parameters used in the conventional CFAR processor can be determined from the presented mathematical description, resulting in the improved detection capability.

This paper is organized as follows. In Section 2, we present the signal model and explain the CFAR processor. Mathematized algorithm parameters are presented with simulation analysis in Section 3. Finally, Section 4 concludes the paper.

2. Signal Model and CFAR Processor

Fig. 1 illustrates a general PCL system. A direct-path signal $r_d(t)$ and a target echo signal $r_t(t)$ can be acquired by using beamforming and adaptive filtering about the received signal at reference and surveillance antenna. These are defined as

$$r_d(t) = a_d s(t - \tau_d), \tag{1}$$

DOI: 10.2316/P.2017.848-045

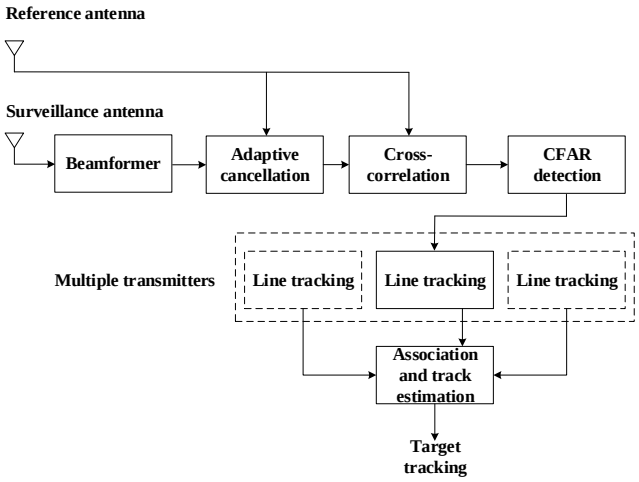

Figure 1. Block diagram of general PCL system.

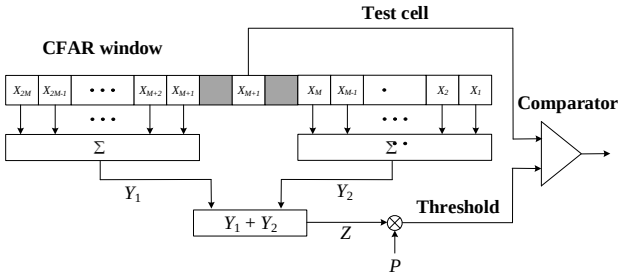

Figure 2. Structure of the CFAR processor.

$$r_t(t) = \sum_{i=1}^{M} a_t^i s(t - \tau_t^i), \tag{2}$$

where M is the number of targets, $s(t)$ is a transmitted signal, a_d and a_t^i are the amplitudes of the received direct-path signal and the ith target echo signal caused by the propagation path loss, respectively. τ_d is the propagation duration of the direct-path from a base station to the PCL receiver and τ_t^i is the propagation time from the base station to the PCL receiver reflected at ith unknown target. Then, the range-Doppler map can be generated by using the direct-path signal and the target echo signal as follows:

$$A(\rho, \nu) = \left| \int_{-\infty}^{\infty} r_d(t) r_t(t + \frac{\rho}{c}) e^{j2\pi\nu t} dt \right|^2, \tag{3}$$

where ρ and ν are independent variable representing the range difference corresponding to time difference and Doppler-frequency difference, respectively.

In order to confirm the existence of multiple unknown targets after calculating the range-Doppler map, the CFAR detection algorithm has to be conducted. The CFAR processor consists of the window cells, the guard cells, and the test cells as shown in Fig. 2. The detection threshold is

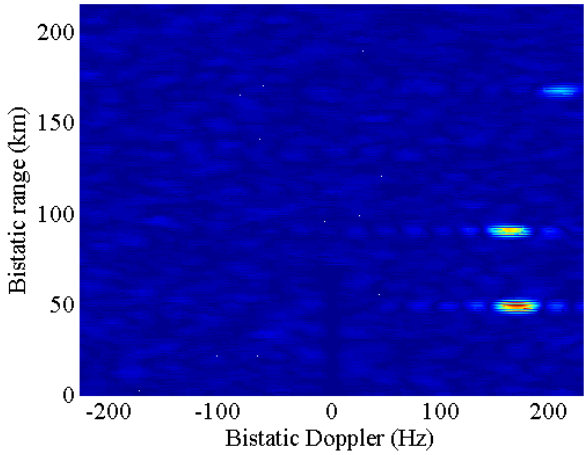

Figure 3. Range-Doppler map based on FM broadcasting signal.

set by the estimated noise power Z which is calculated based on the window cells and the constant factor P calculated by the false alarm probability. Consequently, target decision is carried out by comparing the value of the test cell with the detection threshold as follows:

$$\begin{cases} \text{No target}(H_0), & \text{if } Y < PZ \\ \text{Target present}(H_1), & \text{if } Y \geq PZ \end{cases} \tag{4}$$

where Y is the value of the test cell. Since the input signal of the CFAR processor is composed of the values at all points of the range-Doppler map corresponding to the equation (2), the values are exponentially distributed. Finally, the constant factor P of (4) can be calculated as follows [7]

$$P = \left(P_{fa}\right)^{-\frac{1}{N}} - 1, \tag{5}$$

where P_{fa} is the false alarm probability and N is the number of reference window cells.

3. Window and Guard Cell Determination

3.1 Selecting a range or Doppler axis of CFAR processor

To determine which axis we will use for the CFAR processor, in this subsection, we analyze the range-Doppler map based on FM signals in terms of guard cell size. For numerical evaluation, we used a stereo FM signal [8], the number of targets of M=3, sampling frequency of f_s=250 kHz, collection time of T=40 ms and the location of the unknown targets, the base station and the PCL receiver are given in table I.

Fig. 3 shows the range-Doppler map obtained with the above simulation parameters and Fig. 4 shows the slice of (a) the Range-Doppler map along the range axis; and (b) the Doppler axis. We approximately marked the region including the mainlobe and sidelobe with a black

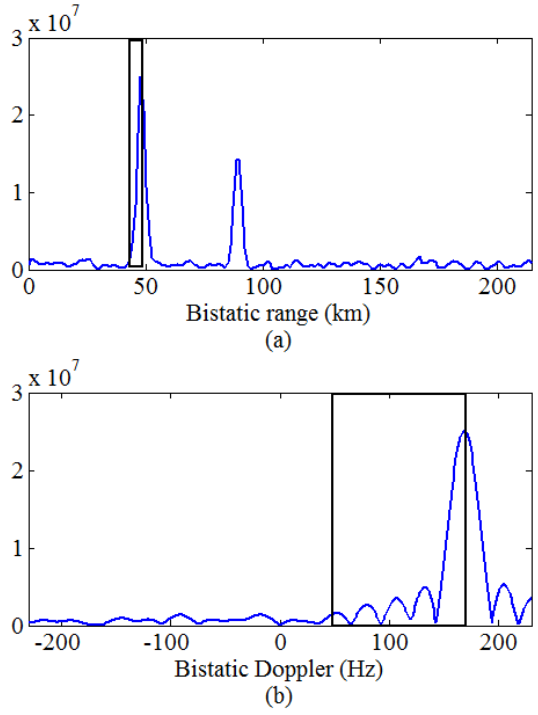

Figure 4. The slices of the range-Doppler map along the range axis (a) and Doppler axis (b).

rectangular box. As shown in Fig. 4, the width along the Doppler axis in (b) is longer than that along the range axis in (a). This width can be reduced by increasing a collection time due to the characteristic that the width of map in (b) is inversely proportional to the collection time [9]. Although the sidelobe along the Doppler axis in Fig. 4(b) can be reduced, however, it cause a computational burden caused by the increased collection time. On the other hand, the sidelobe of the range-Doppler map along the range axis (a) does not exist. Also, the narrow mainlobe in the range axis is fixed because the width of this mainlobe is inversely proportional to the bandwidth of the input signal of the range-Doppler map [9] and the bandwidth of the commercial FM signal is fixed of 75 kHz. Consequently, we have to conduct the CFAR processor along the range axis.

3.2 Determination of the Window and Guard Cell Sizes

In this subsection, we present the proper window size and guard cell size on the CFAR processor for the PCL systems based on the FM signal.

Table 1. The position and velocity of the receiver and targets

Object	Position	Velocity
Transmitter	[50 0 0]^T km	Stationary
Receiver	[-50 0 0]^T km	Stationary
Target A	[30 50 0]^T km	[-150 -320 0] m/s
Target B	[-10 80 0]^T km	[-150 -320 0] m/s
Target C	[60 110 0]^T km	[-150 -320 0] m/s

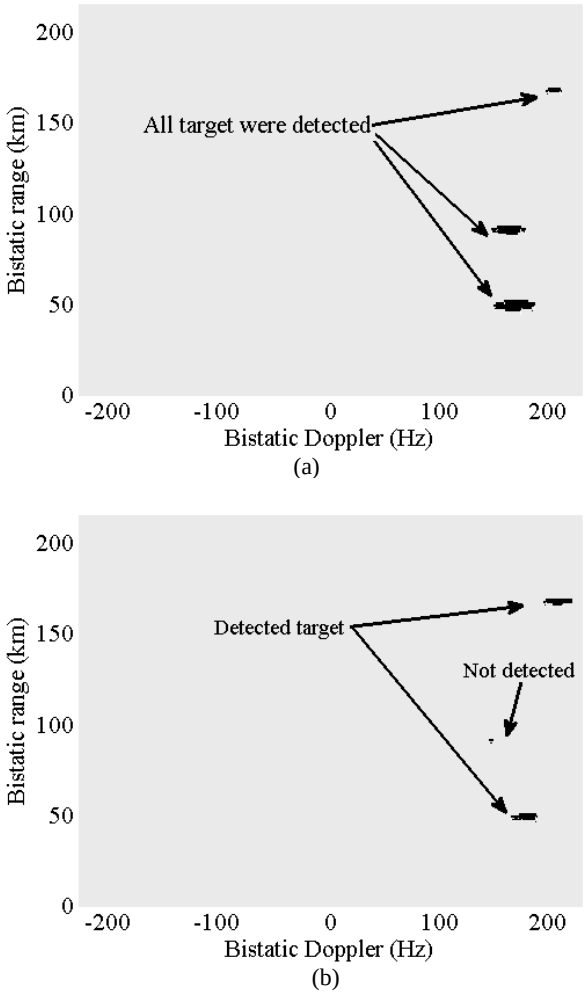

Figure 5. The results of the CFAR proceesor with the range-Doppler map according to the window size: (a) 30 (b) 10.

the mainlobe along the Doppler axis of the range-Doppler First, the guard cell can be determined from Fig. 4(a). As we explained in 3.1, the width of mainlobe is inversely proportional to the bandwidth of the FM signal. Thus, to acquire the exact noise power from window cell removing the near value of the peak points which is caused by targets, guard cell size can be determined by dividing the width of mainlobe into sampling time as follows:

$$N_G = \lceil (1/B)\, f_s \rceil \tag{5}$$

where $\lceil x \rceil$ is a smallest integer that is larger than or equal to x, B is the bandwidth of the FM signal. From the equation (5), the value of guard cell N_G is 4 when we used parameters which is presented above.

Fig. 5 show the result of the CFAR processor with the range-Doppler map corresponding to Fig. 3. Here, Fig. 5(a) and (b) show the results when the window size is 10 30, respectively. While the peak point at (90 km, 163 Hz) on range-Doppler map is detected by the processor as shown in Fig. 5(a), not detected when the window size is assigned by 30 as shown in Fig. 5(b). Under the circumstance for Fig. 5(b), the threshold large which is

determined by the estimated noise power from the window cells is too high because the window cells of the CFAR processor include the several points near the peak point which is caused by the target A when the test cell is the peak point by target B. Consequently, the resolution ΔR which distinguish between adjacent targets is determined by converting the sum of the number of window and guard cells into distance unit as follows:

$$\Delta R = \left(N_W + N_G \right) c T_s \tag{6}$$

where N_W is the window size, c is propagation velocity and T_s is sampling time. Thus, window cell size can be calculated after the bistatic range resolution is determined. For example, if the bistatic resolution is determined as 25 km, the window cell size can be assigned as 16 with the same parameters set in 3.1.

4. Conclusion

We presented how to use a CFAR detector in a PCL system using FM broadcasting signals. Firstly, the algorithm parameters of the number of window cells and that of guard cells for the CFAR processor were mathematically derived based on the range-Doppler map. While adjacent multiple targets could be successfully detected by using the adequate algorithm parameters chosen based on our mathematical derivation, one target was missed when the arbitrary value were used. We also found that the bistatic range axis is better than the Doppler axis due to the sidelobe effect in terms of estimation accuracy. It is expected that our presented results will be very helpful for determining the design parameters of a PCL system using FM broadcasting signals.

Acknowledgement

This work was supported by LIG Nex1 Co., Ltd [A research on PCL localization technique, Y16-009]

References

[1] A. A. Konovalov, Target tracking algorithm for passive coherent location, IET Radar, Sonoar and Navigation, *10*(7), 2016, 1228-1233.

[2] D. Pastina, F. Colone, T. Martelli and P. Falcone, Parasitic exploitation of Wi-Fi signals for indoor radar surveillance, *IEEE Transactions on Vehicular Technology*, *64*(4), 2015, 1401-1415.

[3] A. Macera, M. Caruso, C. Bongioanni, E. Anniballi, R. Cardinali, Civil air traffic surveillance with passive radar for anti-terrorism, *2012 Tyrrhenian Workshop on Advances in Radar and Remote Sensing(TyWRRS)*, 2012, 296-303.

[4] M. Malanowski, K.S. Kulpa, P. Samczynski, J. Misiurewicz and J. Kulpa, Long range FM-based passive radar, *Conference on IET International Radar Systems(Radar 2012)*, 2012, 1-4.

[5] P. E. Howland, D. Maksimiuk and G. Reitsma, FM radio based bistatic radar, *IEE Proceeding on Radar Sonar and Navigation 3*, 2005, 107-115.

[6] F. Colone, D. W. O'hagan, P. Lombardo and C. J. Baker, A multistage processing algorithm for disturbance removal and target detection in passive bistatic radar, *IEEE Transactions on Aerospace and Electronic Systems*, *45*(2), 2009, 698-722.

[7] H. Rohling, Radar CFAR thresholding in clutter and multiple target situations, *IEEE Transactions on Aerospace and Electronic Systems*, *AES-19*(4), 1983, 608-621.

[8] A. Lauri, F. Colone, R. Cardinali, C. Bongioanni, and P. Lombardo, Analysis and emulation of FM radio signals for passive radar, *in IEEE Aerospace Conference*, 2007, 1-10.

[9] X. Hu, Computing the Cross Ambiguity Function, Master's thesis, Dept. Electrical Engineering, Binghamton Univ., New York, 2005.